HYDROLOGICAL PROCESSES
*Hydrol. Process.* **24**, 1660–1671 (2010)
Published online 26 April 2010 in Wiley InterScience
(www.interscience.wiley.com) DOI: 10.1002/hyp.7677

# Generality of fractal 1/f scaling in catchment tracer time series, and its implications for catchment travel time distributions

Sarah E. Godsey,[1]* Wenche Aas,[2] Thomas A. Clair,[3] Heleen A. de Wit,[4] Ivan J. Fernandez,[5] J. Steve Kahl,[6] Iain A. Malcolm,[7] Colin Neal,[8] Margaret Neal,[8] Sarah J. Nelson,[6] Stephen A. Norton,[9] Marisa C. Palucis,[1] Brit Lisa Skjelkvåle,[4] Chris Soulsby,[10] Doerthe Tetzlaff[10] and James W. Kirchner[1,11]

[1] *Department of Earth & Planetary Science, University of California—Berkeley, Berkeley, CA 94720-4767, USA*
[2] *NILU, Dept. Atmospheric and Climate Research, P.O. Box 100, 2027 Kjeller, Norway*
[3] *Water Science and Technology Br., Environment Canada, PO Box 6227, Sackville, N.B., E4L 1G6, Canada*
[4] *Norwegian Institute for Water Research (NIVA), Gaustadalléen 21, 0349 Oslo, Norway*
[5] *The University of Maine, 5722 Deering Hall, Orono, ME 04469-5722, USA*
[6] *Senator George J. Mitchell Center for Environmental and Watershed Research, 5710 Norman Smith Hall, University of Maine, Orono, ME 04469-5710, USA*
[7] *Marine Scotland, Freshwater Laboratory, Faskally, Pitlochry PH16 5LB, UK*
[8] *Centre for Ecology and Hydrology, Wallingford, Oxfordshire OX10 8BB, UK*
[9] *Department of Earth Sciences, and the Climate Change Institute, University of Maine, Orono, ME 04469-5790, USA*
[10] *Northern Rivers Institute, School of Geosciences, University of Aberdeen, Aberdeen AB24 3UF, UK*
[11] *Swiss Federal Institute for Forest, Snow, and Landscape Research (WSL), Birmensdorf, Switzerland; Department of Environmental Sciences, Swiss Federal Institute of Technology (ETH), Zurich, Switzerland*

## Abstract:

Catchment travel time distributions reflect how precipitation from different storms is stored and mixed as it is transported to the stream. Catchment travel time distributions can be described by the mean travel time and the shape of the distribution around the mean. Whereas mean travel times have been quantified in a range of catchment studies, only rarely has the shape of the distribution been estimated. The shape of the distribution affects both the short-term and long-term catchment response to a pulse input of a soluble contaminant. Travel time distributions are usually estimated from conservative tracer concentrations in precipitation and streamflow, which are analyzed using time-domain convolution or spectral methods. Of these two approaches, spectral methods are better suited to determining the shape of the distribution. Previous spectral analyses of both rainfall and streamflow tracer time series from several catchments in Wales showed that rainfall chemistry spectra resemble white noise, whereas the stream tracer spectra in these same catchments exhibit fractal 1/f scaling over three orders of magnitude. Here we test the generality of the observed fractal scaling of streamflow chemistry, using spectral analysis of long-term tracer time series from 22 catchments in North America and Europe. We demonstrate that 1/f fractal scaling of stream chemistry is a common feature of these catchments. These observations imply that catchments typically exhibit an approximate power-law distribution of travel times, and thus retain a long memory of past inputs. The observed fractal scaling places strong constraints on possible models of catchment behavior, because it is inconsistent with the exponential travel time distributions that are predicted by simple mixing models. Copyright © 2010 John Wiley & Sons, Ltd.

KEY WORDS travel-time distribution; tracer; mixing; lakes; transit time

*Received 31 August 2009; Accepted 25 February 2010*

## INTRODUCTION

Catchment storage and mixing of solutes can be characterized by the catchment travel time distribution, which is defined by both the mean travel time and the shape of the distribution around the mean. Catchment responses to contamination or land use change, as well as biogeochemical responses linked to hydrological processes (Rodhe *et al.*, 1996; Wolock *et al.*, 1997; Landon *et al.*, 2000; Burns *et al.*, 2005; Turner *et al.*, 2006; Tetzlaff *et al.*, 2007), depend in part on the travel-time distribution. The mean travel-time describes the aggregate average flushing rate of the catchment, whereas the shape of the distribution is determined by the heterogeneity of the flowpath lengths and velocities. Quantifying this heterogeneity is crucial to understanding how streams respond to rainfall and how long water-borne contaminants might persist in the catchment (e.g. Kirchner *et al.*, 2000).

Catchment travel times are typically modeled with the exponential distribution, a special case of the gamma family of distributions, expressed in a simplified form as

$$h(\tau) = \frac{1}{\tau_o} e^{-\tau/\tau_o} \quad (1)$$

*Correspondence to: Sarah E. Godsey, Pennsylvania State University, Department of Civil and Environmental Engineering, University Park, PA 16802. E-mail: seg19@psu.edu

where $\tau$ is the time for an individual parcel of tracer to reach the stream after falling as precipitation, and $\tau_o$ is the mean travel time. The exponential travel-time distribution assumes that the catchment behaves as a single linear well-mixed reservoir (McGuire *et al.*, 2005). The exponential distribution scales with the mean travel time $\tau_o$, and has a particular shape within the broader family of gamma distributions. That broader family of gamma distributions,

$$h(\tau) = \frac{\tau^{\alpha-1}}{\beta^{\alpha}\ \Gamma(\alpha)} e^{-\tau/\beta} = \frac{\tau^{\alpha-1}}{(\tau_o/\alpha)^{\alpha}\ \Gamma(\alpha)} e^{-\alpha\tau/\tau_o} \qquad (2)$$

can take on a wide range of shapes as its shape factor $\alpha$ varies, including distributions that are strongly peaked at short time and have long tails (for small values of its shape factor $\alpha$), as well as distributions that rise to a peak and then decline, resembling a typical storm hydrograph (for larger values of $\alpha$), as shown in Figure 1. The gamma distribution subsumes the exponential distribution as a special case when its shape factor $\alpha$ equals to 1. Besides the shape factor $\alpha$, the only other parameter in the gamma distribution is the mean travel time $\tau_o$, or alternatively the scale factor $\beta = \tau_o/\alpha$. The incomplete gamma function $\Gamma(\alpha)$ serves as a normalization constant, making the area under the distribution equal to 1. The $\beta$-form of the gamma distribution is commonly found in the statistical literature, but the equivalent $\tau_o$-form is also given in Equation (2) to make its dependence on mean travel time explicit and to allow direct comparison with the exponential distribution in Equation (1). The shape factor in the gamma distribution controls how much weight is found in the tails of the distribution, versus near the centre, reflecting the heterogeneity in the catchment flowpath lengths and velocities. The smaller the value of $\alpha$, the greater the variability in travel times compared to the mean; in fact, the coefficient of variation of the gamma distribution (the ratio of the standard deviation to the mean) equals the square root of $1/\alpha$. Following an analysis showing that some catchments are characterized by gamma travel-time distributions with shape factors near $\alpha = 0{\cdot}5$ (Kirchner *et al.*, 2000), several physical interpretations of this behavior have been proposed, including advection and dispersion of spatially distributed inputs (Kirchner *et al.*, 2001), variable subsurface advection (Lindgren *et al.*, 2004) and multiple well-mixed linear or coupled nonlinear reservoirs in series and in parallel (Shaw *et al.*, 2006).

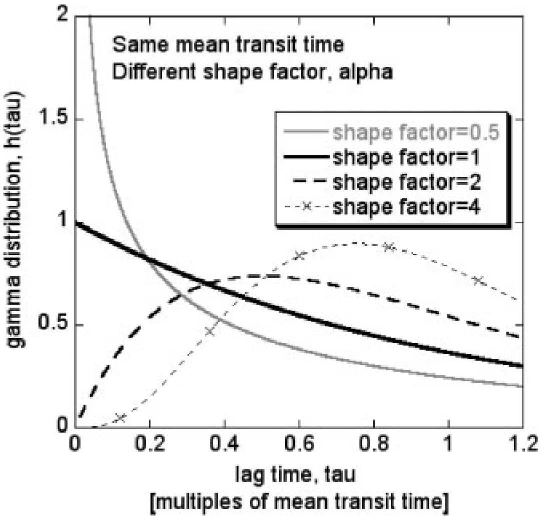


Figure 1. Comparison of gamma distributions of travel times for different shape factors ($\alpha = 0{\cdot}5$, 1, 2 and 4) as a function of lag time, expressed as a multiple of mean transit time. The shape factor of 1 is a special case of the gamma distribution and is equivalent to the exponential distribution

Although other catchment travel time distributions are used, by far the most commonly employed is the exponential travel time distribution. It was used in 66% of the catchment travel time distribution models reviewed by McGuire and McDonnell (2006), whereas gamma distributions (except for the special case of the exponential distribution) were used in only approximately 2% of those studies. Other theoretical models that yield power-law travel time distributions sometimes exhibit means and other moments that are infinite (e.g. Cvetkovic and Haggerty, 2002; Scher *et al.*, 2002). These imply that there is an infinite accumulation of tracers in catchments which is not supported by field evidence, and therefore we do not consider these models further in this work. Other distributions, including the sine-wave, exponential-piston flow, dispersion, piston flow and binomial models, have also been used in catchment travel time distribution studies. Here, we consider only the gamma model, including the special case of the exponential model, because the exponential model is used more commonly than all other models combined, and the wide range of possible shapes of the gamma distribution encompasses shapes similar to many other possible catchment travel time distributions.

Kirchner *et al.* (2000, 2001) showed that in a series of Welsh catchments, the gamma travel time distribution with $\alpha \approx 0{\cdot}5$ better reproduced the power spectral scaling of the catchments' tracer time series than the exponential distribution did. Here, we test whether this behaviour is particular to the Welsh catchments, or whether these gamma distributions represent travel time distributions in other catchments as well. The distinction between different distribution shapes is particularly important when we consider how a catchment would flush out a pulse of a soluble contaminant (Figure 2). The smaller the value of $\alpha$, the greater the intensity of contamination in the stream in the short term, and the greater the persistence of the contaminant in the stream in the long term (Figure 2). Thus, both the short- and long-term implications of contamination episodes will be underestimated if exponential distributions are mistakenly assumed to govern catchments that instead obey gamma distributions with $\alpha < 1$.

Here, we analyse tracer time series from 22 diverse catchments to determine whether the exponential model accurately represents their travel-time behavior. Characteristics of our study catchments are summarized in Table I. The study sites are generally small headwater catchments, with drainage areas ranging from 0·3

 

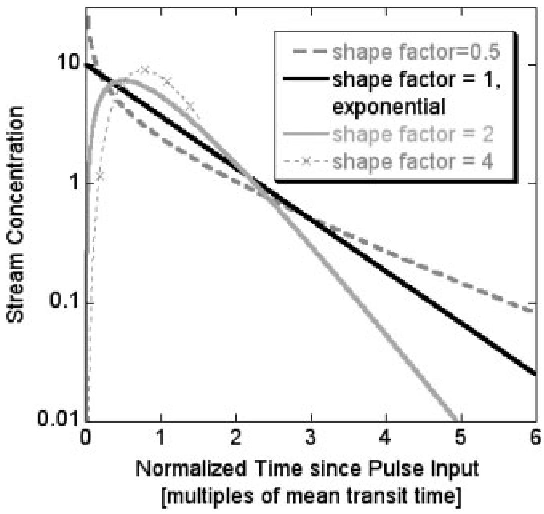


Figure 2. Recovery time series of the concentration of a hypothetical soluble contaminant introduced in a pulse of 10 arbitrary units at time zero. The exponential model (solid black) shows a slow initial recovery relative to the low shape factor gamma model (dashed grey) and a faster recovery compared to the gamma model with shape factors above 1 (solid and dotted grey). After approximately three times the mean transit time, the contaminant shows more long-term persistence for gamma models with shape factors below 1 than would be expected if the exponential model described the catchment behaviour. Gamma models with shape factors larger than 1 recover more quickly than the exponential model would predict, with concentrations that are approximately 10× lower after four mean transit times have elapsed

to 295 km$^2$ (median 1·6 km$^2$) and average catchment slopes ranging from approximately 2–16 degrees. Gage elevation ranges from sea level to 580 m. Soil types include gleysols, histosols and podzols, and the bedrock lithologies of the catchments include metamorphic and granitic rocks, as well as sandstones and shales. All sites were affected by Pleistocene glaciation, and saprolite was removed from most sites during that period. Vegetative cover varies across the catchments: most are forested to some extent, and several have been felled or burned at some point in the past 50–100 years. The catchments are typically sampled weekly and the record length varies from 4 to 29 years. This study focuses on catchments in maritime settings, with chloride deposition fluxes that are large compared to observed or estimated rates of biogeochemical cycling in soils and vegetation, so that chloride can be plausibly used as a tracer of hydrologic mixing and storage. Likewise, the study catchments are temperate and generally humid (mean annual precipitation is approximately 1450 mm/yr, with one site as low as 350 mm/yr, and most between 685 and 3900 mm/yr), limiting the potential effect of evapoconcentration on the stream chloride time series. We discuss the use of chloride, each site's mass balance, and the relevance of conservative tracers for this analysis below.

## METHODS

We analysed chloride tracer time series in precipitation and streamflow for each site using spectral methods. We used spectral methods rather than the more commonly used time domain convolution methods (McGuire and McDonnell, 2006) because it can be difficult to distinguish between exponential and non-exponential gamma models in the time domain (Figure 3), but they appear distinct when analysed with spectral techniques (Figure 4).

For all catchments in this study, we used the longest time series of chloride concentrations in precipitation and streamflow that were available (see Table I for the record length at each site). Chloride was used because it is more widely available than other potential conservative tracers such as deuterium or $^{18}$O. A conservative tracer is one which reacts or fractionates slowly enough that it reflects the mixing processes of the system of interest (Turner and Barnes, 1998). If this is the case, the chloride tracer moves with the water, and mixing of waters of different ages will lead to damping of chloride fluctuations in the output (streamflow) relative to the input (precipitation) across a range of time scales. Concern about whether chloride is a sufficiently conservative tracer (Bastviken *et al.*, 2006) encouraged us to limit our analysis to sites where chloride input fluxes are high enough that reactions in the soil should be small in comparison. To check whether this was sufficient, we also estimated the chloride mass balance on an annually averaged basis for each site (Table II). We calculated the annual average chloride mass fluxes as the product of annual water fluxes in precipitation or streamflow and annual average concentration in precipitation and streamflow, respectively. Average annual mean concentrations are calculated as numerical rather than volume-weighted mean concentrations. Chloride mass fluxes in precipitation and stream water are within 10% of each other at seven sites, and within 50% of one another at all but two sites (Cadillac and Hadlock streams; see Results and Discussion Section for more information about these sites). At two sites (Mharcaidh and Svarttjern), chloride inflows exceeded outflows. This may be due to retention of inputs, or the mass balance may reflect an error due to underestimation of discharge, overestimation of chloride inputs, or sampling bias affecting the averaged results. Particularly at the Mharcaidh, chloride inputs may be overestimated due to extensive sampling at lower elevations and lower Cl concentrations at higher elevations. Unfortunately, mass balance can be difficult to achieve in many field studies which employ natural or artificial tracers, and the accuracy of mass flux estimates can be influenced by non-stationarity of inputs, non-representative samples (e.g. due to the type or size of precipitation sampler) and short records (where the tail of the distribution is never measured).

For each site, the precipitation or streamflow time series was truncated so that both would cover the same span of time. The inverse of this time span is the so-called fundamental frequency. Spectral power was measured at all integer multiples of this fundamental frequency, up to the Nyquist frequency. Because some of the time series were unevenly sampled and all had occasional missing data, the Nyquist frequency was estimated from

 

Table I. Site information for the 22 catchments included in this study

| Region | Stream and precipitation site names (Citations in superscripts) | Catchment outlet locations (dd.ddd) Latitude | Catchment outlet locations (dd.ddd) Longitude | Precipitation gage location (dd.ddd) Latitude | Precipitation gage location (dd.ddd) Longitude | Catchment area ($km^2$) | Mean annual precipitation (mm) | Mean annual flow (mm) | Catchment outlet elevation (m) | Lake above catchment outlet? | Mean catchment slope (degrees) | Soil type/description |
|---|---|---|---|---|---|---|---|---|---|---|---|---|
| Central Scotland | Loch Ard B10/Loch Ard[a] | 56·157 | −4·465 | 56·085 | −4·293 | 0·9 | 2000 | 1660 | 170 | No | 11 | Hydrologically responsive soils (Gleysols) |
| Central Scotland | Loch Ard B11/Loch Ard[a] | 56·157 | −4·464 | 56·085 | −4·293 | 1·4 | 2000 | 1670 | 170 | No | 9 | Hydrologically responsive soils (Gleysols, Peats) |
| Maine | Cadillac/NADP ME98[c,j] | 44·345 | −68·216 | 44·377 | −68·261 | 0·316 | 1332 | 968 | 122 | No | 16·26 | Thin Spodosols over till, or Histosols |
| Maine | Hadlock/NADP ME98[b] | 44·332 | −68·279 | 44·377 | −68·261 | 0·472 | 1332 | 1110 | 137 | No | 11·54 | Thin Spodosols over till, or Histosols |
| N Scotland | Mharcaidh/Mharcaidh[d] | 57·070 | −3·510 | 57·056 | −3·494 | 10 | 1200 | 850 | 330 | No | 15 | Freely draining alpine soils (30%) Humus Iron Podzols (35%), hydrologically responsive soils (Peats, 25%) |
| Norway | Birkenes/Birkenes[e] | 58·384 | 8·239 | 58·383 | 8·25 | 0·41 | 1400 | 1136 | 200 | No | n/a | Podzols (90%), Peats (7%) |
| Norway | Dalelva/Karpbukt (also Karpdalen)[f] | 69·685 | 30·386 | 69·667 | 30·367 | 3·2 | 350 | 497 | 0 | Yes | n/a | Leptosols (61%), Podzols (20%), Peats (4%) |
| Norway | Kaarvatn/Kaarvatn[e] | 62·780 | 8·891 | 62·783 | 8·883 | 25 | 1450 | 1843 | 200 | Yes | n/a | Bare rock and Leptosols (76%), Podzols (20%), Peats, 2% |
| Norway | Langtjern Inlet/Gulsvik[e] | 60·371 | 9·732 | 60·367 | 9·65 | 1 | 685 | 595 | 510 | No | n/a | Leptosols (74%), Podzols (5%), Peats (16%) |
| Norway | Langtjern/Gulsvik[e] | 60·372 | 9·727 | 60·367 | 9·65 | 4·8 | 685 | 595 | 510 | Yes | n/a | Leptosols (74%), Podzols (5%), Peats (16%) |
| Norway | Oygardsbekken/Skreadalen (also Ualand)[f] | 58·622 | 6·107 | 58·817 | 6·717 | 2·55 | 2140 | 1546 | 185 | No | n/a | Leptosols (83%), Podzols (4%), Peats (6%) |
| Norway | Storgama/Treungen[e] | 59·052 | 8·654 | 59·017 | 8·517 | 0·6 | 960 | 956 | 580 | Yes | n/a | Bare rock and Leptosols (59%), Peats (22%), Podzols (11%) |
| Norway | Svarttjern/Haukeland[g] | 60·831 | 5·568 | 60·817 | 5·583 | 0·57 | 3900 | 2848 | 302 | Yes | n/a | Podzols (68%), bare rock and Leptosols (17%) |
| Norway | Trodola/Nausta[h] | 61·578 | 5·941 | 61·577 | 5·898 | 10 | 2388 | 2864 | n/a | No | n/a | Leptosols and Podzols |
| Nova Scotia | Mersey/Kejimkujik[i] | 44·437 | −65·223 | 44·434 | −65·206 | 295 | 1450 | 866 | 109 | Yes | 2·48 | Shallow sandy loam, till |
| Nova Scotia | Moose Pit/Kejimkujik[i] | 44·462 | −65·048 | 44·434 | −65·206 | 17 | 1352 | 851 | 103 | No | 2·60 | Shallow sandy loam, till |
| Nova Scotia | Pine Marten/Kejimkujik[i] | 44·424 | −65·213 | 44·434 | −65·206 | 1·3 | 1352 | 850 | 114 | No | 3·33 | Shallow sandy loam, till |
| Wales | Hafren/Plynlimon[c,k] | 52·475 | −3·705 | 52·47[p] | −3·71[p] | 3·47 | 2378 | 2092 | 300 | No | 3·41 | Peaty podzols and gleys |
| Wales | Hore/Plynlimon[c,k] | 52·471 | −3·705 | 52·47[p] | −3·71[p] | 3·35 | 2378 | 1884 | 300 | No | 4·04 | Peaty podzols and gleys |
| Wales | Tanwyllth/Plynlimon[c,k] | 52·474 | −3·706 | 52·47[p] | −3·71[p] | 0·51 | 2378 | 4331 | 400 | No | 7·13 | Sandy podzols and gleys |
| Wales | Upper Hafren/Plynlimon[c,k] | 52·487 | −3·727 | 52·47[p] | −3·71[p] | 1·17 | 2378 | 2000[m] | 500 | No | n/a | Sandy podzols and gleys |
| Wales | Upper Hore/Plynlimon[c,k] | 52·470 | −3·722 | 52·47[p] | −3·71[p] | 1·78 | 2378 | 1950 | 500 | No | n/a | Sandy podzols and gleys |

Table I. (*Continued*)

| Stream and Precipitation Site Names | Geological Description | Vegetation | Land Cover Change | Stream Record | | Ppt Record | | Other notes | Drainage Density |
|---|---|---|---|---|---|---|---|---|---|
| Citations in superscripts | | | | Start date | End date for this analysis | Start date | End date for this analysis | | (km/km$^2$) |
| Loch Ard B10/Loch Ard[a] | Quartz-rich metamorphics, glacial till | Forest plantation | Felling in parts in 1988/89, 2003/04/05 | 1988 | 2005* | 1988 | 2006* | Validated based on field surveys and OS maps, generally at 10-m resolution | 2.82 |
| Loch Ard B11/Loch Ard[a] | Quartz-rich metamorphics, glacial till | Forest plantation | Felling in parts in 1997/98/99, 2003/04/05 | 1988 | 2005* | 1988 | 2006* | Validated based on field surveys and OS maps, generally at 10-m resolution; same rain gauge as for Loch Ard B10 | 2.87 |
| Cadillac/NADP ME98[c,j] | Cadillac Granite bedrock of Devonian age | 60% Open/shrub/scrub; 20% hardwood; 20% coniferous | 'A large portion of this watershed burned severely in 1947 and probably more than once in the 1800s, and has supported heterogeneous successional forests for 200 years or longer'. (Schauffler *et al.*, 2007) | 1999 | 2006 | 1981 | 2003* | MAP based on years for which there is stream data | 2.0-4.1 |
| Hadlock/NADP ME98[b] | Cadillac Granite bedrock of Devonian age | 23% Open/shrub/scrub; 7% hardwood; 70% coniferous | 'The unburned watershed has been dominated by spruce (Picea rubens) and fir (Abies balsamea) for 500 years or more and has not recently burned or been substantially cleared'. (Schauffler *et al.*, 2007) | 1999 | 2006 | 1981 | 2003* | MAP based on years for which there is stream data | 2.4-5.3 |
| Mharcaidh/Mharcaidh[d] | Granite (with extensive drift) | Heather peatland (60%), montane rock (34%), rest conifers | Tree cover currently expanding due to reduced grazing by red deer (Cervus elaphus) | 1985 | 2001* | 1985 | 2001* | Validated based on field surveys and OS maps, generally at 10-m resolution | 2.14 |
| Birkenes/Birkenes[e] | Glaciated, granite, biotite | Norway spruce | Felling of forest at 7% of catchment in 1985, otherwise no changes | 1972 | 2006* | 1977 | 2006* | | n/a |
| Dalelva/Karpbukt (also Karpdalen)[f] | Glaciated, gneiss and other metamorphic rocks | Birch | Mature forest, no direct anthropogenic influences | 1988 | 2006* | 1998 (1990 for Karpdalen) | 2006* (1998 for Karpdalen) | | n/a |
| Kaarvatn/Kaarvatn[e] | Glaciated, gneiss and quartsite | Montane rock, heather, pine, birch | Mature forest, no direct anthropogenic influences | 1978 | 2006* | 1978 | 2006* | | n/a |
| Langtjern Inlet/Gulsvik[e] | Glaciated, gneiss | Pine forest, spruce forest, peat | Mature forest, no direct anthropogenic influences | 1973 | 2000* | 1980 | 1997 | Elevation estimated as equal to that at Langtjern | n/a |
| Langtjern/Gulsvik[e] | Glaciated, gneiss | Pine forest, spruce forest, peat | Mature forest, no direct anthropogenic influences | 1973 | 2006* | 1980 | 1997 | | n/a |

Table I. (*Continued*)

| Stream and Precipitation Site Names<br>Citations in superscripts | Geological Description | Vegetation | Land Cover Change | Stream Record | | Ppt Record | | Other notes | Drainage Density |
|---|---|---|---|---|---|---|---|---|---|
| | | | | Start date | End date for this analysis | Start date | End date for this analysis | | (km/km$^2$) |
| Oygardsbekken/Skreadalen (also Ualand)[f] | Glaciated, gneiss, mignatites | Montane rock, heather, pine, birch | Mature forest, no direct anthropogenic influences | 1992 | 2006* | 1980 (1991 for Ualand) | 2005* (2000 for Ualand) | | n/a |
| Storgama/Treungen[e] | Glaciated, granite, biotite | Montane rock, heather, pine, birch | Mature forest, no direct anthropogenic influences | 1974 | 2006* | 1977 | 2006* | | n/a |
| Svarttjern/Haukeland[g] | Glaciated, gneiss | Pine forest | Mature forest, no direct anthropogenic influences | 1994 | 2006* | 1981 | 2006* | | n/a |
| Trodola/Nausta[h] | Glaciated, gneiss and other metamorphic rocks | Forest | Mature forest, no direct anthropogenic influences | 1984 | 2004 | 1985 | 2006 | | n/a |
| Mersey/Kejimkujik[i] | Greywacke, sandstone | Spruce, fir, pine, maple, birch, beech, oak | Maturing forest | 1980 | 2007 | 1983 | 2004* | Wetland veg in <1%, drainage density map resolution = 20m | 1.08 |
| Moose Pit/Kejimkujik[i] | Greywacke, sandstone | Spruce, fir, pine, maple, birch | Maturing forest | 1983 | 2007 | 1983 | 2004* | Wetland veg in <1%, drainage density map resolution = 20 m | 0.90 |
| Pine Marten/Kejimkujik[i] | Greywacke, sandstone | Spruce, fir, pine, maple, birch | Maturing forest | 1990 | 2007 | 1983 | 2004* | Drainage density map resolution = 20 m | 1.11 |
| Hafren/Plynlimon[c,m] | Lower Paleozoic shales, mudstones, sandstones | Sitka spruce | Afforested and actively managed forest planted on moorland/pastures in the 1930s | 1983 | 2007* | 1983 | 2007* | Outlet elevation estimated from CEH map for Plynlimon sites | n/a |
| Hore/Plynlimon[c,m] | Lower Paleozoic shales, mudstones, sandstones | Sitka spruce | Afforested and actively managed forest planted on moorland/pastures in the 1930s | 1983 | 2007* | 1983 | 2007* | | n/a |
| Tanwyllth/Plynlimon[c,m] | Lower Paleozoic shales, mudstones, sandstones | Sitka spruce | Afforested and actively managed forest planted on moorland/pastures in the 1930s | 1991 | 2007* | 1983 | 2007* | | n/a |
| Upper Hafren/Plynlimon[c,m] | Lower Paleozoic shales, mudstones, sandstones | Sitka spruce | Afforested and actively managed forest planted on moorland/pastures in the 1930s | 1990 | 2007* | 1983 | 2007* | | n/a |
| Upper Hore/Plynlimon[c,m] | Lower Paleozoic shales, mudstones, sandstones | Sitka spruce | Afforested and actively managed forest planted on moorland/pastures in the 1930s | 1984 | 2007* | 1983 | 2007* | | n/a |

References are as follows: a = Tetzlaff *et al*., 2007; b = Kahl *et al*., 2007; c = Brandt *et al*., 2004; d = Soulsby *et al*., 2000; e = De Wit *et al*., 2008; f = Kaste *et al*., 2004; g = SFT, 2007; h = Hindar *et al*., 2004; i = Yanni *et al*., 2000; j = Schauffler *et al*., 2007; k = Neal and Kirchner, 2000. P = reported precipitation values and chemistry from an average of 40 gages located throughout the catchment. K = Upper Hafren mean annual flow is estimated. Asterisk indicates that precipitation or streamflow chemistry sampling is ongoing.

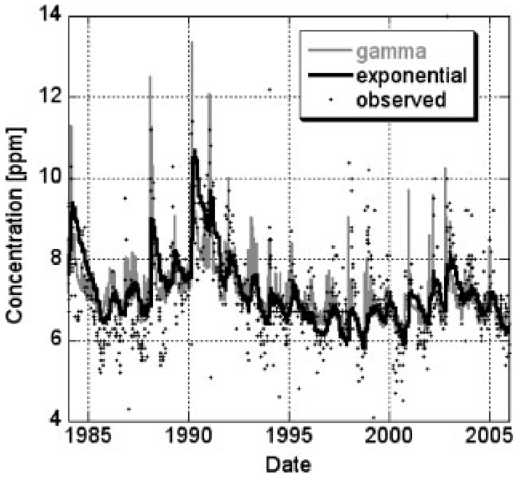


Figure 3. Time series of measured (black dots) and modelled (lines) tracer concentrations in Hafren stream, one of the study sites. The modelled concentrations result from the convolution in the time domain of observed rainfall concentrations and the best-fit exponential (solid black, Equation 1) or gamma (solid grey, Equation 2) travel time distribution. The parameters in those equations are varied such that the modeled and measured concentrations match as accurately as possible in a least squares sense. It can be difficult to distinguish among different models in the time domain, but these same models can be shown to be significantly different in the spectral domain (Figure 4)

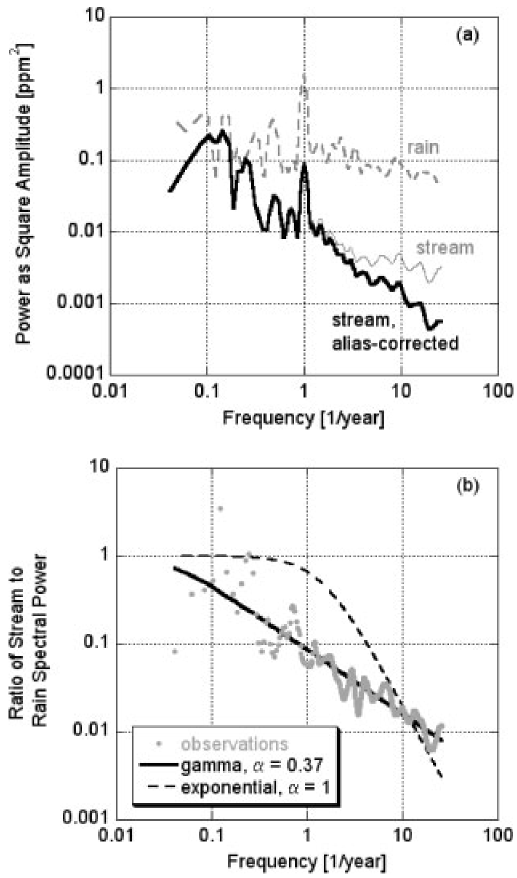


Figure 4. (a) Power spectra versus frequency for the input rainfall concentrations and output stream concentrations, showing the effect of alias-corrections at Hafren stream, one of the study sites. The ratio of the stream spectral power to rain spectral power equals the transfer function. (b) Power spectra versus frequency plot showing the best-fit exponential and gamma travel time distributions in the spectral domain and the transfer function at Hafren. At the data-rich high frequencies, the differences between the spectra of the two travel-time distributions are clear, with the gamma distribution corresponding more closely to the transfer function

the median interval between samples. We calculated the spectral power for the rainfall and stream time series at each of these frequencies using the date-compensated discrete Fourier transform (DCDFT) method proposed by Ferraz-Mello (1981) and further elaborated by Foster (1996), because it avoids a potentially serious artifact that can arise in the better-known Lomb-Scargle Fourier Transform (Foster, 1995). We band-averaged the resulting power spectra with a triangular smoothing window with a width of approximately 0·1 log units in frequency (as shown in the top plot in Figure 4).

We filtered the resulting spectra to correct for the effects of aliasing, in which spectral power above the Nyquist frequency appears instead as spurious spectral power below the Nyquist frequency. Aliasing can lead to artificially shallow spectral slopes, particularly with power-law spectra such as those analysed here (Kirchner, 2005). To account for possible aliasing effects, we passed these results through an aliasing filter with an assumed corner frequency of 1 h, and a limiting frequency of twice the minimum (fundamental) frequency (Kirchner, 2005). We then calculated the ratio of the spectral power of the stream tracer time series to that of the precipitation tracer, to obtain the so-called transfer function (e.g. lower plot in Figure 4). The transfer function is useful because the convolution theorem says that if the stream concentrations are determined by the convolution of the precipitation concentrations and a travel-time distribution, then the power spectrum of that travel-time distribution equals the transfer function (see Kirchner *et al.*, 2001 for details). The power spectrum of the gamma distribution is, from Equation (2):

$$|H(f)|^2 = \left(1 + (2\pi\ f\ \tau_o/\alpha)^2\right)^{-\alpha} \quad (3)$$

(Bain, 1983). From Equation (3), one can see that at frequencies that are high compared to $\alpha/\tau_o$, the spectrum of the transfer function should follow a power law with a slope of approximately $-2\alpha$. Thus, a first estimate of $\alpha$ can be obtained directly from the power-law slope of the transfer function, or equivalently, from the difference between the power-law slopes of the tracer spectra in streamflow and precipitation. To estimate the best-fit gamma travel-time distribution for each of the sites, we fitted Equation (3) to each site's empirical transfer function. We adjusted the parameters of the hypothetical travel time distributions to minimize the sum of squared differences between the hypothetical and the empirical transfer function power spectra in logarithmic space.

## RESULTS AND DISCUSSION

Gamma distribution shape factors could be estimated for 20 of our 22 sites (all except Cadillac and Hadlock Brooks). At all 20 sites, the shape factor $\alpha$ was significantly less than 1, implying that the exponential distribution does not accurately represent the mixing behavior

 

Table II. Summary of the average annual precipitation amount [mm], streamflow [mm], and Cl concentrations [mg/L], and calculated annual average chloride mass fluxes in precipitation and streamflow [Mg/km$^2$/yr] for each study catchment

| Region | Stream and precipitation site names (Citations in superscripts) | Mean annual precipitation (mm) | Mean annual flow (mm) | Avg annual precipitation concentration (mg/L) | Avg annual stream concentration (mg/L) | Precipitation mass flux (Mg/km$^2$/yr) | Stream mass flux (Mg/km$^2$/yr) | Ratio of precipitation : stream fluxes (%) |
|---|---|---|---|---|---|---|---|---|
| Central Scotland | Loch Ard B10/Loch Ard[a] | 2000 | 1660 | 3·29 | 6·20 | 6·6 | 10·3 | 64 |
| Central Scotland | Loch Ard B11/Loch Ard[a] | 2000 | 1670 | 3·29 | 8·00 | 6·6 | 13·4 | 49 |
| Maine | Cadillac/NADP ME98[c,j] | 1332 | 968 | 1·05 | 5·44 | 1·4 | 5·3 | 27 |
| Maine | Hadlock/NADP ME98[b] | 1332 | 1110 | 1·05 | 5·65 | 1·4 | 6·3 | 22 |
| N Scotland | Mharcaidh/Mharcaidh[d] | 1200 | 850 | 3·25 | 3·55 | 3·9 | 3·0 | 129 |
| Norway | Birkenes/Birkenes[e] | 1400 | 1136 | 2·52 | 4·61 | 3·5 | 5·2 | 67 |
| Norway | Dalelva/Karpbukt (also Karpdalen)[f] | 350 | 497 | 6·10 | 4·09 | 2·1 | 2·0 | 105 |
| Norway | Kaarvatn/Kaarvatn[e] | 1450 | 1843 | 2·27 | 2·05 | 3·3 | 3·8 | 87 |
| Norway | Langtjern Inlet/Gulsvik[e] | 685 | 595 | 0·50 | 0·69 | 0·3 | 0·4 | 84 |
| Norway | Langtjern/Gulsvik[e] | 685 | 595 | 0·50 | 0·60 | 0·3 | 0·4 | 96 |
| Norway | Oygardsbekken/Skreadalen (also Ualand)[f] | 2140 | 1546 | 3·06 | 6·98 | 6·5 | 10·8 | 61 |
| Norway | Storgama/Treungen[e] | 960 | 956 | 0·82 | 1·13 | 0·8 | 1·1 | 73 |
| Norway | Svarttjern/Haukeland[g] | 3900 | 2848 | 3·53 | 3·46 | 13·8 | 9·9 | 140 |
| Norway | Trodola/Nausta[h] | 2388 | 2864 | 1·99 | 2·90 | 4·8 | 8·3 | 57 |
| Nova Scotia | Mersey/Kejimkujik[i] | 1450 | 866 | 3·18 | 5·62 | 4·6 | 4·9 | 95 |
| Nova Scotia | Moose Pit/Kejimkujik[i] | 1352 | 851 | 3·18 | 3·61 | 4·3 | 3·1 | 140 |
| Nova Scotia | Pine Marten/Kejimkujik[i] | 1352 | 850 | 3·18 | 4·36 | 4·3 | 3·7 | 116 |
| Wales | Hafren/Plynlimon[c,k] | 2378 | 2092 | 3·93 | 7·09 | 9·3 | 14·8 | 63 |
| Wales | Hore/Plynlimon[c,k] | 2378 | 1884 | 3·93 | 7·59 | 9·3 | 14·3 | 65 |
| Wales | Tanwyllth/Plynlimon[c,k] | 2378 | 2208 | 3·93 | 7·81 | 9·3 | 17·3 | 54 |
| Wales | Upper Hafren/Plynlimon[c,k] | 2378 | 2000[m] | 3·93 | 5·80 | 9·3 | 11·6 | 80 |
| Wales | Upper Hore/Plynlimon[c,k] | 2378 | 1950 | 3·93 | 7·38 | 9·3 | 14·4 | 65 |

The average Cl concentrations are numerical means rather than volume-weighted means. The ratio of the precipitation to stream mass fluxes is also listed, with 100% indicating equal inflows and outflows. Superscripts are as indicated in the caption for Table I.

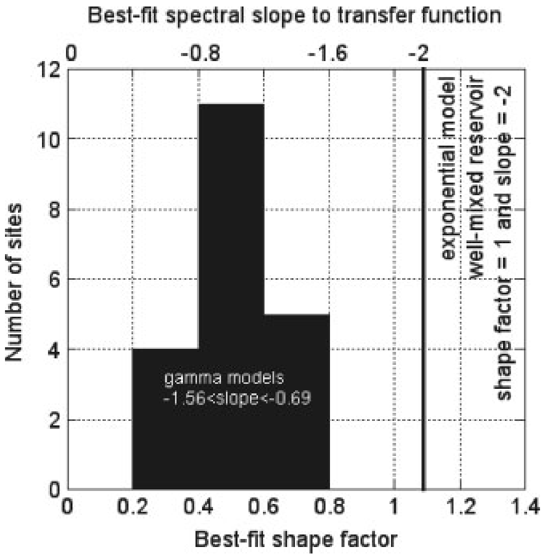


Figure 5. Distribution of best-fit shape factors (lower $x$-axis) and corresponding high-frequency transfer function slopes (upper $x$-axis) for 20 catchments in this study. None of the shape factors are as large as 1, the shape factor that would imply an exponential travel time distribution accurately describes the mixing and storage processes. Instead, they cluster around a shape factor of 0·5 and range within a relatively narrow band from 0·35 to 0·78. More weight of the travel time distribution is found in the tails of the distribution, implying that flowpaths and timing is more heterogeneous than an exponential model would predict

of any of these catchments (Figure 5 and Table III). The best-fit transfer function slopes ranged from −0·69 to −1·56, implying shape factors ranging from 0·35 to 0·78. None of the transfer functions were as steep as a slope of −2, which would correspond to an exponential travel time distribution. This implies that the exponential travel time distribution, and its assumption of a well-mixed linear reservoir, does not describe catchment behaviour. Instead, most catchments appear to exhibit more heterogeneous behavior with a wider range of flowpaths and travel times (shape factors less than 1), leading to more weight in the tails of the travel time distribution. Thus, in most catchments, a pulse input of a soluble contaminant would produce a sharper short-term peak in stream concentrations, and more persistent long-term contamination, than would be predicted from an exponential travel time distribution.

Although all slopes are shallower than −2, implying greater heterogeneity than predicted by an exponential model, the spectral slopes vary from site to site. Sites with a shallower slope, such as Upper Hafren and Dalelva, have more weight in the tails of the modelled travel time distribution. These sites would be expected to have some precipitation which very quickly reaches the stream as well as some very long slow flowpaths.

On the other hand, several sites have spectral slopes that are relatively steep, implying shape factors closer to 1. Four of the five sites with the steepest transfer function spectral power slopes—and thus with travel time distributions that are closest to exponential—have lakes in them (Figure 6). We would expect that lakes would act like true mixing tanks. True mixing tanks should exhibit an exponential travel time distribution (a shape factor of 1), and we see that most catchments with lakes have shape factors >0·6 (Figure 6). The Langtjern Inlet and Outlet sites are at the inlet and outlet of the Langtjern Lake, respectively. Thus, they should offer a clear comparison of the effects of lake mixing on

Table III. Summary of best-fit travel time distribution parameters based on fitting Equation (3) to the calculated transfer function power spectra. Typical mean transit times are less than 1 year, and typical shape factors are approximately 0·5

| Site name | Alpha | Alpha s.e. | Mean transit time (yr) | Mean transit time s.e. |
|---|---|---|---|---|
| Dalelva/Karpbukt[a] | 0·35 | 0·01 | 2·91 | 0·42 |
| Upper Hafren/Plynlimon | 0·35 | 0·01 | 4·44 | 0·39 |
| Hafren/Plynlimon | 0·37 | 0·00 | 1·62 | 0·09 |
| Hore/Plynlimon | 0·38 | 0·00 | 0·70 | 0·03 |
| Oygardsbekken/Skreadalen[b] | 0·44 | 0·04 | 0·09 | 0·01 |
| Upper Hore/Plynlimon | 0·47 | 0·00 | 0·42 | 0·01 |
| Tanwyllth/Plynlimon | 0·48 | 0·01 | 0·23 | 0·01 |
| Mharcaidh/Mharcaidh | 0·49 | 0·00 | 1·22 | 0·05 |
| Pine Marten/Kejimkujik | 0·51 | 0·01 | 0·49 | 0·03 |
| Langtjern Outlet/Gulsvik | 0·52 | 0·01 | 0·73 | 0·03 |
| Loch Ard B10/Loch Ard | 0·56 | 0·02 | 0·08 | 0·00 |
| Moose Pit/Kejimkujik | 0·57 | 0·01 | 0·61 | 0·03 |
| Trodola/Nausta | 0·58 | 0·01 | 0·28 | 0·01 |
| Birkenes/Birkenes | 0·58 | 0·01 | 0·16 | 0·00 |
| Loch Ard B11/Loch Ard | 0·60 | 0·02 | 0·05 | 0·00 |
| Svarttjern/Haukeland | 0·62 | 0·01 | 0·18 | 0·01 |
| Kaarvatn/Kaarvatn | 0·65 | 0·01 | 0·23 | 0·00 |
| Mersey/Kejimkujik | 0·69 | 0·01 | 0·35 | 0·01 |
| Langtjern Inlet/Gulsvik | 0·73 | 0·01 | 0·10 | 0·00 |
| Storgama/Treungen | 0·78 | 0·01 | 0·08 | 0·00 |
| Cadillac/NADP ME98 | —[c] | — | — | — |
| Hadlock/NADP ME98 | —[c] | — | — | — |

Footnotes are as follows: a = similar results obtained for Karpdalen precipitation record; b = similar results obtained for Ualand precipitation record; c = quantities could not reasonably be determined.

 

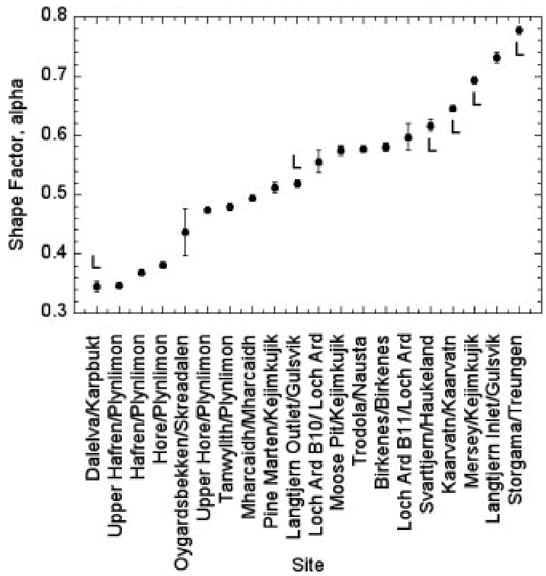


Figure 6. Estimates of the shape factor for each site and its associated uncertainty, sorted from lowest to highest estimates. Lakes (indicated with an L) are more likely to be found within the catchment boundaries of the sites with larger shape factors

the travel time distribution shape factor, but several factors may obscure this relationship. First, low chloride concentrations affected by detection limits create a 'floor' in the spectrum which may obscure possible steepening of the Langtjern Outlet spectrum relative to the Langtjern Inlet spectrum. Second, the Langtjern Inlet samples only a small portion of the total inlet catchment area, so that it does not just exclude the lake mixing itself. Broadly, the catchments in which there are no lakes have significantly smaller shape factors than those in which there are lakes. This method successfully reflects the impact of lakes on the mixing processes occurring within the catchment boundaries.

Other site characteristics (except for the presence or absence of lakes) do not appear to be correlated with variations in the shapes of the travel-time distributions across our study sites. In other studies, mean travel time has been found to be related to site hillslope gradient, mean hillslope length, and soil permeability classifications (McGlynn *et al.*, 2003; McGuire *et al.*, 2005; Hrachowitz *et al.*, 2009; Tetzlaff *et al.*, 2009). Across our 22 sites, gamma distribution shape factors and mean transit times are not significantly correlated with any of the site characteristics listed in Table I. One would expect catchment geometry and soil and geological characteristics to influence the heterogeneity of subsurface flowpaths and thus the shape of the travel-time distribution, but such an effect may not be strong enough to be seen in our data. In particular, many of the site characteristics in Table I are similar within each region, such that the effective number of substantially different sites is smaller than the total of 22 sites in our analysis. All sites were affected by Pleistocene glaciation, implying that transmissivity through permeable bedrock is diminished due to saprolite removal. Flowpaths in unglaciated regions with more permeable bedrock would be expected to vary even more widely, and thus be less likely to correspond to exponential travel time distributions.

Our analysis has considered only the family of gamma distributions, in comparison with the special case of the exponential distribution, which is widely assumed to describe catchment behavior (but which, as shown above, is inconsistent with the spectral scaling observed in the chloride tracer time series analysed here). Other commonly used travel-time models are also inconsistent with the spectral behavior of our 22 sites. The exponential-piston flow model, for example, has the same transfer function as the exponential distribution, and thus does not match the spectral behavior of our sites any better. Dispersion models exhibit even steeper spectral scaling than the exponential distribution (Kirchner *et al.*, 2000), and so are even less compatible with the spectral behavior we have observed. We have also considered whether the estimated shape factor and scaling relationships leading to these inferences are predictably corrupted by the distance from mass balance. No significant relationship is seen between the best-fit shape factor (Table III) and the ratio of chloride inflows to outflows (Table II), suggesting that closer mass balance would not systematically alter the estimate of the distribution shape.

Although the spectral analysis method works well, some conditions can lead to problematic calculations of spectral signature. At Loch Ard B10 and B11, Oygaards-bekken and Pine Marten, for example, many of the sampling intervals are at weekly, biweekly or monthly intervals, that is, integer multiples of the median sampling frequency. Sampling at such intervals can lead to a partial violation of the Nyquist theorem, resulting in falsely inflated power at the high-frequency end of the spectrum. Such sampling patterns are common, and should be considered during the interpretation of the results of spectral analysis. In these cases, we split the records into shorter subsets (often with one predominant sampling interval) and re-ran the analyses. Because we observed the same spectral pattern in the shorter records, we have more confidence in the accuracy of the inferred travel time distributions. At the two sites in Maine, Cadillac and Hadlock Brooks, the method is unable to produce reasonable estimates of the travel time distribution. At these sites, output spectral power is always higher than the input spectral power, implying that (1) output variability is unusually large, (2) output variability has been amplified or (3) at least one additional chloride input remains unsampled. Mass influxes differed from mass outfluxes by more than 50% at these sites (Table II). Previous atmospheric deposition research at these sites found that Cl in throughfall (an estimate of wet + dry deposition) was 2·2–6·2 times greater than wet-only deposition, and winter deposition of Cl was much greater than that measured during the growing season, because of the marine origin of many winter storms (Nelson, 2007). Accounting for these additional sources and processes leading to the apparent amplification of the output signal is necessary in order to accurately estimate the travel time distribution.

 

## CONCLUSION

The shape of the catchment travel-time distribution reflects the integrated catchment response to water inputs, and in turn, many soluble contaminants. The shape of the travel time distribution is often assumed to be well represented by an exponential travel time distribution model, but we found that this was inappropriate at all sites for which the travel-time distribution could be estimated because it was inconsistent with observed spectral scaling. The non-exponential gamma model with a shape factor $<1$, implying significant weight in the distribution tails, can be applied at all sites. This implies that there is greater heterogeneity in the travel times of individual water parcels through catchments than would be inferred from the exponential travel time distribution. Catchment with large lakes should behave as large well-mixed reservoirs with shape factors near one, and most of our study sites with shape factors greater than 0·6 had prominent lakes or ponds within the stream network. However, where lakes were absent, the shape factor was not correlated with any other site characteristics. Although further work is needed to clarify how site characteristics influence the shape of the travel time distribution, our work showed that the heavy-tailed non-exponential gamma model could be used to characterize the shape of the travel time distribution at all sites.

ACKNOWLEDGEMENTS

We thank the many field crews and lab technicians who created the data analysed here. Our analysis was supported by NSF grant EAR-0125550 to JWK, by an NSF Graduate Research Fellowship to SEG, and by the Berkeley Water Center. The analysis of Scottish site data was supported by the Leverhulme Trust (F/00152/U). The collection and analysis of the Maine site data were supported by the US EPA, US National Park Service, US Geological Survey, Maine Department of Environmental Protection, and the University of Maine. Data collection in Nova Scotia was funded by Environment Canada.

## REFERENCES

Bain L. 1983. In *Gamma distribution. Encyclopedia of Statistical Sciences*, vol. 3, Kotz S and Johnson NL (eds). Wiley: New York; 292–298.

Bastviken D, Sandén P, Svensson T, Ståhlberg C, Magounakis M, Öberg G. 2006. Chloride retention and release in a boreal forest soil: Effects of soil water residence time and nitrogen and chloride loads. *Environmental Science and Technology* **40**: 2977–2982, DOI: 10.1021/es0523237.

Brandt C, Robinson M, Finch JW. 2004. Anatomy of a catchment: the relation of physical attributes of the Plynlimon catchments to variations in hydrology and water status. *Hydrology and Earth System Science* **8**: 345–354.

Burns D, Vitvar T, McDonnell J, Hassett J, Duncan J, Kendall C. 2005. Effects of suburban development on runoff generation in the Croton River basin, New York, USA. *Journal of Hydrology* **311**: 266–281.

Cvetkovic V, Haggerty R. 2002. Transport with multiple-rate exchange in disordered media. *Physical Review E* **65**: 051308, DOI: 10.1103/PhysRevE.65.051308.

De Wit HA, Hindar A, Hole L. 2008. Winter climate affects long-term trends in stream water nitrate in acid-sensitive catchments. *Hydrology and Earth System Science Discussions* **4**: 3055–3085.

Ferraz-Mello S. 1981. Estimation of periods from unequally spaced observations. *Astronomical Journal* **86**: 619–624.

Foster G. 1995. The CLEANEST Fourier spectrum. *Astronomical Journal* **109**: 1889–1902.

Foster G. 1996. Wavelets for period analysis of unevenly sampled time series. *Astronomical Journal* **112**: 1709–1729.

Hindar A, Tørseth K, Henriksen A, Orsolini Y. 2004. The significance of the North Atlantic oscillation (NAO) for sea-salt episodes and acidification-related effects in Norwegian rivers. *Environmental Science and Technology* **38**: 26–33.

Hrachowitz M, Soulsby C, Tetzlaff D, Dawson JJC, Dunn SM, Malcolm IA. 2009. Using long-term data sets to understand transit times in contrasting headwater catchments. *Journal of Hydrology* **367**: 237–248.

Kahl JS, Nelson SJ, Fernandez I, Haines T, Norton S, Wiersma GB, Jacobson G, Amirbahman A, Johnson K, Schauffler M, Rustad L, Tonnessen K, Lent R, Bank M, Elvir J, Eckhoff J, Caron H, Ruck P, Parker J, Campbell J, Manski D, Breen R, Sheehan K, Grygo A. 2007. Watershed nitrogen and mercury geochemical fluxes integrate landscape factors in long-term research watersheds at Acadia National Park, Maine, USA. *Environmental Monitoring and Assessment* **126**: 9–25. DOI: 10.1007/s10661-006-9328-0.

Kaste O, Rankinen K, Lepisto A. 2004. Modelling the impacts of climate and deposition changes on nitrogen fluxes in northern catchments of Norway and Finland. *Hydrology and Earth System Science* **8**: 778–792.

Kirchner JW, Feng XH, Neal C. 2000. Fractal stream chemistry and its implications for contaminant transport in catchments. *Nature* **403**: 524–527.

Kirchner JW, Feng XH, Neal C. 2001. Catchment-scale advection and dispersion as a mechanism for fractal scaling in stream tracer concentrations. *Journal of Hydrology* **254**: 82–101.

Kirchner JW. 2005. Aliasing in 1/f noise spectra: Origins, consequences, and remedies. *Physical Review E* **71**: 066110.

Landon MK, Delin GN, Komor SC, Regan CP. 2000. Relation of pathways and transit times of recharge water to nitrate concentrations using stable isotopes. *Groundwater* **38**(3): 381–395.

Lindgren GA, Destouni G, Miller AV. 2004. Solute transport through the integrated groundwater-stream system of a catchment. *Water Resources Research* **40**: W03511, DOI:10.1029/2003WR002765.

McGlynn B, McDonnell J, Stewart M, Seibert J. 2003. On the relationships between catchment scale and streamwater mean residence time. *Hydrological Processes* **17**: 175–181.

McGuire KJ, McDonnell JJ, Weiler M, Kendall C, McGlynn BL, Welker JM, Seibert J. 2005. The role of topography on catchment-scale water residence time. *Water Resources Research* **41**: W05002, DOI:10.1029/2004WR003657.

McGuire KJ, McDonnell. 2006. A review and evaluation of catchment transit time modeling. *Journal of Hydrology* **330**: 543–563.

Neal C, Kirchner JW. 2000. Sodium and chloride levels in rainfall, mist, streamwater and groundwater at the Plynlimon catchments, mid-Wales: Inferences on hydrological and chemical controls. *Hydrology and Earth System Science* **8**: 295–310.

Nelson SJ. 2007. Winter contribution to annual throughfall inputs of mercury and tracer ions at Acadia National Park, Maine. Ph.D. Dissertation. University of Maine, Orono, Maine, USA.

Rodhe A, Nyberg L, Bishop K. 1996. Transit times for water in a small till catchment from a step shift in the oxygen 18 content of the water input. *Water Resources Research* **32**: 3497–3511.

Schauffler M, Nelson SJ, Kahl JS, Jacobson GL, Haines TA, Patterson WA, Johnson KB. 2007. Paleoecological Assessment of Watershed History in PRIMENet Watersheds at Acadia National Park, USA. *Environmental Monitoring and Assessment* **126**: 39–53. DOI: 10.1007/s10661-006-9330-6.

Scher H, Margolin G, Metzler R, Klafter J, Berkowitz B. 2002. The dynamical foundation of fractal stream chemistry: The origin of extremely long retention times. *Geophysical Research Letters* **29**: 1061. DOI: 10.1029/2001GL014123.

SFT. 2007. The Norwegian monitoring programme for long-range transported air pollutants. Annual report—Effects 2006 Report TA 2274/2007. The Norwegian Pollution Control Authority (SFT), Oslo, Norway. (In Norwegian).

Shaw SB, Harpold AA, Taylor JC and Walter TM. 2008. Investigating a high resolution, stream chloride time series from the Biscuit Brook catchment, Catskills, NY. *Journal of Hydrology* **348**: 245–256.

Soulsby C, Malcolm R, Helliwell R, Ferrier RC, Jenkins A. 2000. Isotope hydrology of the Allt a Mharcaidh catchment, Cairngorms, Scotland: implications for hydrological pathways and residence times. *Hydrological Processes* **14**: 747–762.

Tetzlaff D, Malcolm IA, Soulsby C. 2007. Influence of forestry, environmental change and climatic variability on the hydrology, hydrochemistry and residence times of upland catchments. *Journal of Hydrology* **346**: 93–111.

Tetzlaff D, Seibert J, McGuire KJ, Laudon H, Burns DA, Dunn SM, Soulsby C. 2009. How does landscape structure influence catchment transit time across different geomorphic provinces?. *Hydrological Processes* **23**: 945–953, DOI: 10.1002/hyp.7240.

Turner J, Albrechtsen HJ, Bonell M, Duguet JP, Harris B, Meckenstock R, *et al* 2006. Future trends in transport and fate of diffuse contaminants in catchments, with special emphasis on stable isotope applications. *Hydrological Processes* **20**: 205–213.

Turner JV and Barnes CJ. 1998. Modeling of isotopic and hydrogeochemical responses in catchment hydrology. In *Isotope Tracers in Catchment Hydrology* Kendall C and McDonnell JJ Elsevier Science BV: Amsterdam; 723–760.

Wolock DM, Fan J, Lawrence GB. 1997. Effects of basin size on low-flow stream chemistry and subsurface contact time in the Neversink River watershed, New York. *Hydrological Processes* **11**: 1273–1286.

Yanni S, Keys K, Clair TA, Arp PA. 2000. Fog and Acidification Impacts on Ion Budgets of Basins in Nova Scotia, Canada. *JAWRA* **36**: 619–631.

 